J Fluoresc (2011) 21:2213–2227
DOI 10.1007/s10895-011-0926-z

ORIGINAL PAPER

Solvent Effect Profiles of Absorbance and Fluorescence Spectra of Some Indole Based Chalcones

Manju Kumari Saroj · Neera Sharma · Ramesh C. Rastogi

Received: 17 May 2011 / Accepted: 28 July 2011 / Published online: 9 August 2011

Abstract The photophysical properties of a series of 3-(1′*H*-Indol-3′-yl)-1-phenylprop-2-en-1-one and its derivatives (indole chalcones) were studied in different solvents. Solvent effects on the absorption and fluorescence spectra were quantified using Reichardt's and bulk solvent polarity parameters and were complemented by the results of the Kamlet-Taft treatment. The observed excited state dipole moment was found to be larger than the ground state dipole moment of these chalcones. The correlation of the solvatochromic Stokes-shifts with the microscopic solvent polarity parameter (E_T^N) was found to be superior to that obtained using bulk solvent polarity functions.

Keywords Dipole moment · Onsager radius · Polarity · Excited state · Solvatochromism

Introduction

Chalcones are a chemical class that shows paramount importance in chemistry and biochemistry [1–5]. They exhibit promising therapeutic efficacy for the treatment of several diseases [6–9]. In addition, chalcones have been extensively used for various optical applications including photo-alignment layer of liquid crystal displays [10–13], photo refractive polymers and fluorescent probes for sensing the DNA [14–16] or metal ions [17–19].

Indole, the potent basic pharmacodynamic nucleus, has been reported to possess a wide variety of biologically active properties, and the substitution of indole ring into the chalcone moiety markedly influences the biological activity of the chalcone. Indole based chalcones show anti-cancer [20], anti-inflammatory [21, 22], neuroprotective [23] and anti-amoebic [24] properties. These compounds have also been investigated as β-amyloid imaging probes [25]. Recent radiation and quantum chemical studies have shown indole chalcones to be the ideal antioxidants [26]. These types of chalcones are also used for the photogeneration of reactive oxygen species and photo-induced plasmid DNA cleavage [27].

The physicochemical and theoretical investigations of indole based chalcones attract special attention towards their excited and ground state properties because of the presence of donor and acceptor moieties in chalcones. The solvent can significantly influence the chemical and physical properties of the solute. The solvents induce changes in the electronic transitions of solutes (solvatochromism) based on the nature and the extent of the solute-solvent interactions in ground and first excited states of solutes (developed locally in the immediate vicinity) [28–30]. The literature related to the systematic solvatochromic study on this system is scarcely available [31]. This paper reports the systematic solvatochromic study of the photophysical properties of some indole based chalcones for the first time. Photophysical studies provide valuable information about ground and excited states, which can be exploited in the determination of excited state dipole moments [32–36], and ground and excited state proton transfer equilibrium reactions in aqueous [37, 38] and micellar media [39–41].

In this paper, solvent effects on the energy of excited and ground states of 3-(1′*H*-Indol-3′-yl)-1-phenylprop-2-en-1-one and its derivatives (Fig. 1) have been investigated by absorption and fluorescence spectroscopy. The photophysical properties of these derivatives in different solvents have been

M. K. Saroj · N. Sharma · R. C. Rastogi (✉)
Department of Chemistry, University of Delhi,
Delhi 110007, India
e-mail: rc.rastogi@gmail.com

Fig. 1 Structure of indole chalcones

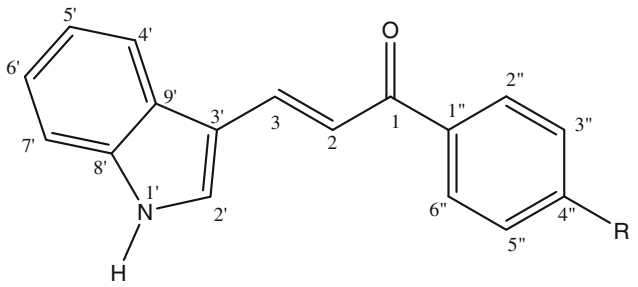

COMPOUNDS	R	Abbreviation
3-(1′*H*-Indol-3′-yl)-1-phenylprop-2-en-1-one	H	I
3-(1′*H*-Indol-3′-yl)-1-p-tolyl-prop-2-en-1-one	CH_3	Me-I
1-(4″-Hydroxy-phenyl)-3-(1*H*-indol-3-yl)-prop-2-en-1-one	OH	OH-I
1-(4″-Chloro-phenyl)-3-(1*H*-indol-3-yl)-prop-2-en-1-one	Cl	Cl-I
3-(1*H*-Indol-3-yl)-1-(4″-methoxyphenyl)-prop -2-en-1-one	OCH_3	OMe-I
3-(1*H*-Indol-3-yl)-1-(4″-nitrophenyl)-prop-2-en-1-one	NO_2	NO_2-I

analyzed using microscopic and bulk solvent polarity parameters and rationalized using the Kamlet-Taft treatment.

Experimental

Materials

Materials and reagents for the synthesis of 3-(1′*H*-indol-3′-yl)-1-phenylprop-2-en-1-one derivatives were purchased from Spectrochem Pvt. Ltd. and used without further purification. All solvents used were of spectroscopic grade (Spectrochem/Merck) and were checked for the absence of absorbing or fluorescent impurities within the scanned spectral ranges. The water used was triple distilled.

Instrumentation

Absorption and fluorescence spectra were recorded by using ANALYTIKA JENA UV WINASPECT SPECTROD PC 250 spectrophotometer and FLUOROMAX SPEX-3 JOBIN YVON HORIBA spectrofluorometer, respectively. All measurements were done in a 1 cm quartz cuvette. Absorption and fluorescence spectra were recorded in freshly prepared 2×10^{-5} M and 1×10^{-5} M solutions, respectively. The slit widths used were 1 nm and 4 nm for absorption and emission measurements, respectively.

Synthesis

The investigated 3-(1′*H*-indol-3′-yl)-1-phenylprop-2-en-1-one derivatives were synthesized according to the procedures reported in the literature [42] and their purity was confirmed by TLC, IR and ^{1}H NMR.

3-(1'H-Indol-3'-yl)-1-Phenylprop-2-en-1-One (I) A solution of indole-3-carboxaldehyde (0.01 mol) and acetophenone (0.01 mol) in 8–10 ml of ethylene glycol was treated with 1 ml of piperidine and refluxed for 20–30 min at 170–180 °C and the progress of reaction was monitored by TLC in ethyl acetate (30%)–petroleum ether (70%) solvent. After cooling the reaction mixture, 5–10 ml of water and 1 ml of glacial acetic acid were added; the crystals that deposited were recrystallized from ethanol. Other derivatives were also synthesized using the same procedure.

Spectral Data

*3-(1'H-Indol-3'-yl)-1-Phenylprop-2-en-1-One (**I**)*

IR (KBr, cm^{-1}): 3428, 3145, 3051, 1640, 1591, 1438, 1367; ^{1}H NMR (400 MHz, DMSO-d_6, ppm): δ7.19–7.22 (d, J = 12 Hz, 1H), 7.44–7.46 (d, J = 8 Hz, 1H), δ7.50–7.55 (m, 2H), δ7.57–7.61 (m, 2H), 7.98 (s, 1H), δ7.99–8.04 (m, 5H), δ11.89 (s, 1H); melting point: 172–174 °C.

*3-(1'H-Indol-3'-yl)-1-p-Tolylprop-2-en-1-One (**Me-I**)*

IR (KBr, cm^{-1}): 3424, 3186, 1638, 1580, 1437, 1355; ^{1}H NMR (400 MHz, DMSO-d_6, ppm): δ2.36 (s, 3H), δ7.17–7.21 (m, 2H), δ7.31–7.33 (d, J = 8 Hz, 1H), δ7.44–7.47 (m, 2H), δ7.58–7.62 (d, J = 16 Hz, 1H), δ7.98 (s, 1H), δ8.00–8.06 (m, 4H), δ11.87 (s, 1H); melting point: 168–170 °C.

*1-(4"-Hydroxyphenyl)-3-(1H-Indol-3-yl)-Prop-2-en-1-One (**OH-I**)*

IR (KBr, cm^{-1}): 3285, 3112, 2927, 1641, 1557, 1440, 1344; ^{1}H NMR (400 MHz, DMSO-d_6, ppm): δ4.57 (s,

1H), δ7.70–7.72 (d, J = 8 Hz, 1H), δ8.01–8.05 (m, 2H), δ8.29–8.31 (m, 2H), δ8.44–8.48 (d, J = 16 Hz, 1H), δ8.78 (s, 1H), δ8.82–8.92 (m, 4H), δ12.68 (s, 1H); melting point: 180–182 °C.

1-(4"-Chlorophenyl)-3-(1H-Indol-3-yl)-Prop-2-en-1-One (**Cl-I**)

IR (KBr, cm^{-1}): 3427, 3186, 1629, 1572, 1435, 1356; ^1H NMR (400 MHz, DMSO-d_6, ppm): δ7.21–7.24 (m, 2H), δ7.47–7.49 (m, 2H), δ7.55–7.57 (d, J = 8 Hz, 1H), δ7.62–7.65 (d, J = 12 Hz, 1H), δ8.02 (s, 1H), δ8.05–8.11 (m, 4H), δ11.91 (s, 1H); melting point: 178–180 °C.

3-(1H-Indol-3-yl)-1-(4"-Methoxyphenyl)-Prop -2-en-1-One (**OMe-I**)

IR (KBr, cm^{-1}): 3389, 3107, 1653, 1601, 1585, 1438, 1360; ^1H NMR (400 MHz, DMSO-d_6, ppm): δ3.80 (s, 3H), δ7.03–7.05 (d, J = 8 Hz, 1H), δ7.18–7.20 (m, 2H), δ7.44–7.45 (m, 2H), δ7.59–7.63 (d, J = 16 Hz, 1H), δ7.96 (s, 1H), δ8.04–8.10 (m, 4H), δ11.83 (s, 1H); melting point: 156–158 °C.

3-(1H-Indol-3-yl)-1-(4"-Nitrophenyl)-Prop-2-en-1-One (**NO_2-I**)

IR (KBr, cm^{-1}): 3368, 3103, 1654, 1559, 1420, 1420, 1341; ^1H NMR (400 MHz, DMSO-d_6, ppm): δ7.22–7.28 (m, 2H), δ7.50–7.52 (m, 2H), δ7.61–7.64 (d, J = 12 Hz, 1H), δ8.09–8.12 (d, J = 12 Hz, 1H), δ8.17 (s, 1H), δ8.31–8.37 (m, 4H), δ12.03 (s, 1H); melting point: 226–228 °C.

Methods

Dipole Moment Calculation

The dipole moment of a molecule in the excited state is determined by the effect of electric field (internal or external) on the position change of the absorption and fluorescence bands. Two methods depending on the internal electric field (solvatochromism) were employed in the present study.

In the first method, by employing the simplest quantum-mechanical second order perturbation theory and taking into account Onsager's model, Kawski et al. [43–51] have obtained the following expressions for $(\overline{\nu}_a - \overline{\nu}_f)$ and 1/2 $(\overline{\nu}_a + \overline{\nu}_f)$:

$$\overline{\nu}_a - \overline{\nu}_f = S_1 F_1(D,n) + C_1 \tag{1}$$

$$1/2\left(\overline{\nu}_a + \overline{\nu}_f\right) = S_2 F_2(D,n) + C_2 \tag{2}$$

where $\overline{\nu}_a$ and $\overline{\nu}_f$ are the absorption and fluorescence maxima, n and D are the refractive index and the dielectric constant of the solvents, respectively. The slopes S_1 and S_2 are expressed as

$$S_1 = \frac{2\left(\mu^* - \mu\right)^2}{hcR^3} \qquad \text{and} \qquad S_2 = \frac{-2\left(\mu^{*2} - \mu^2\right)}{hcR^3} \tag{3}$$

where, μ and μ* are excited and ground state dipole moments of the solute molecule, respectively and 'R' is the Onsager cavity radius. F_1(D,n) and F_2(D,n) are taken as

$$F_1(D,n) = \left[\frac{D-1}{D+2} - \frac{n^2-1}{n^2+2}\right] \times \frac{2n^2+1}{n^2+2} \tag{4}$$

$$F_2(D,n) = \frac{1}{2}F_1(D,n) + \frac{3/2(n^4-1)}{(n^2+2)^2} \tag{5}$$

Plots of the Stokes-shifts $(\overline{\nu}_a - \overline{\nu}_f)$ and $1/2(\overline{\nu}_a + \overline{\nu}_f)$ against the bulk solvent polarity functions, (F_1(D,n) and F_2(D,n)) for different solvents yield the slopes S_1 and S_2, respectively. Assuming that the angle between μ and μ* is small and the cavity radius, 'R' is same in both the ground and the excited states and using the Eqs. 1, 2 and 3, the ratio of the dipole moments in the excited and ground states, which is given by the equation:

$$\frac{\mu^*}{\mu} = \frac{|S_1 - S_2|}{|S_1 + S_2|} \tag{6}$$

It may be noted that most theories [52–57] of the solvent effect on the location of the absorption $(\overline{\nu}_a)$ and fluorescence $(\overline{\nu}_f)$ bands lead, in spite of different assumptions, to similar expressions for $\overline{\nu}_a - \overline{\nu}_f$ and $1/2(\overline{\nu}_a + \overline{\nu}_f)$ (Eqs. 1 and 2) with the difference, however, that the applied solvent polarity parameters, (F_1(D,n) and F_2(D,n)) differ significantly.

In the second method [58], the problem associated with the error in estimating the Onsager radius 'R' was minimized, since the ratio of two Onsager radii (R_B/R) is involved Eq. 7. The excited-state dipole moment is determined by

$$\Delta\overline{\nu}_{af} = 11307.6\left[(\Delta\mu/\Delta\mu_B)^2(\mathrm{R_B/R})^3\right]E_T^N + \text{constant} \tag{7}$$

where $\Delta\overline{\nu}_{af}$ is the Stokes-shifts and E_T^N is the solvent-polarity parameter proposed by Reichardt [59], that correlates better than the traditionally used bulk solvent polarity functions. E_T^N is based on the absorption wave-number of a standard betaine dye in the solvent. Its value for different solvents is given in Table 1 and is expressed as

$$E_T^N = \frac{E_T(solvent) - E_T(TMS)}{E_T(water) - E_T(TMS)} \tag{8}$$

Table 1 Various solvent parameters used in the solvatochromic studies

Solvent	$E_T(30)$ kcal/mol	E_T^N	$F_1(D,n)$	$F_2(D,n)$	α	β	π*
n-Hexane	31.0	0.009	−0.003	0.254	0.00	0.00	−0.011
Cyclohexane	30.9	0.006	−0.003	0.288	0.00	0.00	0.000
1,4-Dioxane	36.0	0.164	0.041	0.307	0.00	0.37	0.490
THF	37.4	0.207	0.549	0.551	0.00	0.55	0.550
Ethyl acetate	38.1	0.228	0.489	0.498	0.00	0.45	0.450
DCM	40.7	0.309	0.590	0.583	0.13	0.10	0.730
DMF	43.2	0.386	0.836	0.710	0.00	0.69	0.880
tert-Butanol	43.3	0.389	0.688	0.608	0.42	0.93	0.410
Acetonitrile	45.6	0.460	0.859	0.664	0.19	0.40	0.660
2-Propanol	48.4	0.546	0.779	0.646	0.76	0.84	0.480
1-Butanol	49.7	0.586	0.750	0.647	0.84	0.84	0.470
Ethanol	51.9	0.654	0.813	0.653	0.83	0.77	0.540
Methanol	55.4	0.762	0.855	0.651	0.98	0.66	0.600
Ethylene glycol	56.3	0.790	0.836	0.710	0.90	0.52	0.920
Water	63.1	1.000	0.913	0.683	1.17	0.47	1.090

$\Delta\mu_B$ (=9D) and R_B (= 6.2Å) are the dipole-moment changes upon excitation and the Onsager cavity radius, respectively, of betaine dye [59, 60], whereas Δμ and 'R' are the corresponding quantities for the molecule of interest (indole chalcones). Thus, the plot of $\Delta\overline{\nu}_{af}$ (Stokes-shifts) versus E_T^N (Eq. 7) can be used to obtain the change in the dipole moment (Δμ) upon excitation.

Parametric Method 3 (PM3) semiempirical molecular-orbital calculations were carried out to obtain the optimized geometries of all the chalcone molecules studied here. The Onsager cavity radii of all molecules have been taken to be 40% of the longest axis in the optimized geometry [61]. The quantum chemical package HyperChem Release 5.1 Pro [62] was used for the semiempirical molecular-orbital calculations.

Kamlet-Taft Treatment: Solvatochromic Comparison

To find the information about the individual contribution of different solvent effects, a multiparametric approach, known as solvatochromic comparison method or linear solvation energy relationship (LSER) proposed by Kamlet, Taft and others [63, 64], has been used. In the general expression (9),

$$\nu = \nu_o + s\left(\pi^* + d\delta\right)\pi^* + a\alpha + b\beta \tag{9}$$

where $\boldsymbol{\nu_o}$ is the vapor phase wave-number (independent of solvent effects) and the values of **ν** are absorption/fluorescence band maxima in a solvent. The empirical parameters **π***, **α** and **β** are a measure of the polarity/polarizability character of the solvent, its hydrogen-bond donor (HBD) and hydrogen-bond acceptor (HBA) capacities, respectively [65–67]. The coefficients **s**, **a** and **b** are interpreted as solute properties. The coefficient, **s** is related to the solute polarity/polarizability character, **a** describes its tendency to accept hydrogen bond from the solvent and **b** measures its property to donate hydrogen bond to the solvent. The coefficients **s**, **a** and **b** indicate the susceptibility of **ν** to a change in the corresponding parameter.

The term **δ** used in Eq. 9 is a 'polarizability correction term', whose value depends on the class of solvents used; for aromatic solvents δ=1, for polyhalogenated solvents δ=0.5 and for all other solvents δ=0 [68]. The term **d** is interpreted as an indicator of the change in direction of the molecular dipole moment in going from initial to transition state, is zero for all spectra that are shifted bathochromically with increasing solvent dipolarity [69]. So, the Kamlet and Taft Eq. 9 reduces to Eq. 10.

$$\nu = \nu_o + s\pi^* + a\alpha + b\beta \tag{10}$$

The corresponding parameters for different solvents were taken from literature [59, 70] and are given in Table 1. All least-squares fit analyses were carried out with Microsoft EXCEL.

Results and Discussion

Absorption and Emission Properties

Absorption and fluorescence spectra of 3-(1′*H*-indol-3′-yl)-1-phenylprop-2-en-1-one (**I**) and its derivatives were recorded in solvents of different polarity. Absorption and fluorescence spectra of **I** in different solvents are shown in Fig. 2 and the corresponding spectral data of all **I** derivatives have been summarized in Tables 2 and 3.

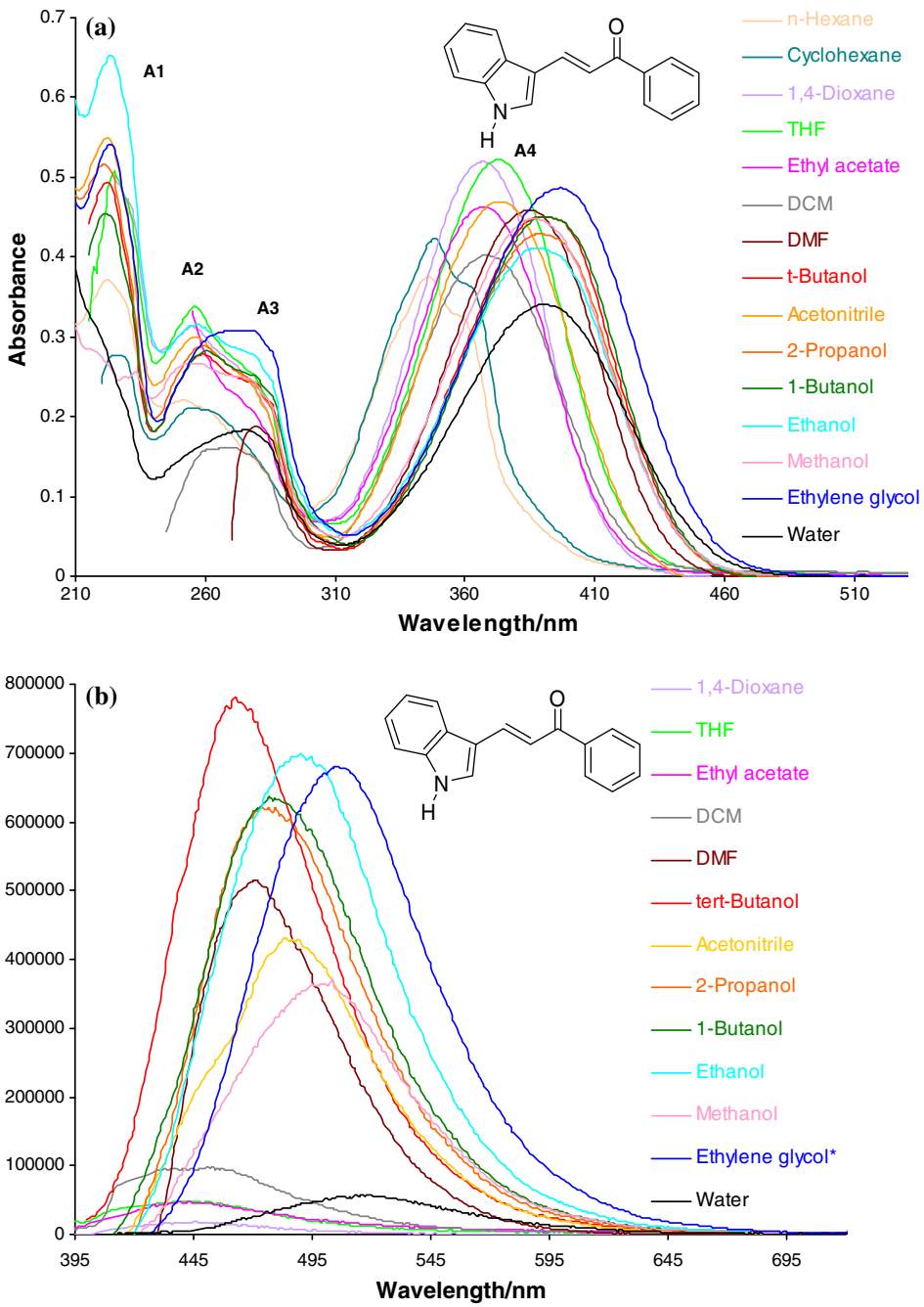

Fig. 2 **a** Electronic absorption spectra of **I** in different solvents. **b** Fluorescence emission spectra of **I** in different solvents. * Fluorescence intensity = 650,000× 2

Absorption Properties

The absorption spectra of all 3-(1′*H*-indol-3′-yl)-1-phenyl-prop-2-en-1-one derivatives consist of four absorption bands (Fig. 2a) (Table 2). It can be clearly seen from the Figs. 2a, 3a and b that the third absorption band (A3) is merging with the second absorption band (A2) and appears as shoulders. However, the first band (A1) and fourth band (A4) appear clearly as distinct absorption bands in all the solvents.

Band A1 is located in the range 220–230 nm in all the derivatives and does not show any change towards the polarity of the solvent as well as the various substituents on the phenyl ring. Absorption band A4 (~340–400 nm) shows a large bathochromic shift (30–55 nm, Table 2) with increase in polarity. Bands A2 and A3 (~250–285 nm) show the less sensitivity towards both solvent polarity and the substituents, as compared to band A4 (Table 2).

The wavelengths, λ_{A1}, λ_{A2} and λ_{A3} of the derivatives are the characteristic absorption bands of the benzoyl group and the indole moiety due to π–π* transitions [71, 72]. The wavelength, λ_{A4} that shows the large bathochromic shift indicates the charge-transfer (CT) interaction among the indole, phenyl and α, β-unsaturated ketone parts of the

Table 2 Absorption maxima of indole chalcone derivatives in different solvents

Solvent[a]	I				Me-I				OH-I				Cl-I				OMe-I				NO_2-I			
	λ_{A1} (in nm)	λ_{A2}	λ_{A3}	λ_{A4}	λ_{A1} (in nm)	λ_{A2}	λ_{A3}	λ_{A4}	λ_{A1} (in nm)	λ_{A2}	λ_{A3}	λ_{A4}	λ_{A1} (in nm)	λ_{A2}	λ_{A3}	λ_{A4}	λ_{A1} (in nm)	λ_{A2}	λ_{A3}	λ_{A4}	λ_{A1} (in nm)	λ_{A2}	λ_{A3}	λ_{A4}
n-Hexane	223	252	269	346	225	267	–	344	NS[b]	NS	NS	NS	223	266	–	352	226	279	297	342	225	268	–	378
Cyclohexane	225	254	–	348	226	269	–	346	NS	NS	NS	NS	224	268	–	354	228	282	295	345	225	274	–	382
1,4-Dioxane	224	255	–	367	226	273	–	366	229	286	300	362	226	270	–	376	228	284	303	364	227	278	313	393
THF	225	255	–	374	–	275	–	370	232	285	300	366	–	–	–	386	229	285	300	368	228	279	319	402
Ethyl acetate	–	–	–	367	–	272	–	366	–	284	298	362	–	–	–	378	–	283	300	364	–	277	322	396
DCM	–	–	268	368	–	275	–	367	–	284	300	365	–	271	–	377	–	285	302	366	–	278	319	396
DMF	–	–	279	385	–	280	–	383	–	288	303	376	–	288	–	393	–	285	302	380	–	282	323	412
tert-Butanol	223	259	281	389	223	279	–	385	224	286	301	390	221	271	–	402	225	286	305	392	223	276	324	418
Acetonitrile	222	256	–	373	223	274	–	372	233	284	298	370	222	267	–	382	226	284	302	372	221	277	320	400
2-Propanol	223	260	–	389	220	279	–	388	229	286	300	390	221	269	–	399	227	286	305	387	225	278	321	418
1-Butanol	222	260	282	391	223	280	–	393	226	286	300	392	222	274	–	400	225	286	306	395	222	276	321	420
Ethanol	225	258	282	388	223	279	–	387	237	286	301	388	223	273	–	396	225	286	304	393	223	276	–	416
Methanol	225	255	–	386	220	279	–	385	229	285	301	385	220	272	–	392	224	285	305	388	220	277	–	411
Ethylene glycol	–	275	–	397	225	281	–	397	231	286	304	395	225	278	–	401	230	286	305	396	228	279	328	421
Water	220	275	–	391	221	279	–	392	228	285	–	393	226	281	–	407	225	285	309	393	222	278	–	416

[a] Solvents are listed in order of increasing dielectric constant values

[b] Not soluble in this solvent

Table 3 Fluorescence maxima of indole chalcone derivatives in solvents of different polarities

Solvent[a]	Fluorescence maximum (λ_{Flu}/nm)					
	I	Me-I	OH-I	Cl-I	OMe-I	NO_2-I[d]
n-Hexane	NF[b]	NF	NS[c]	NF	NF	NS
Cyclohexane	NF	NF	NS	NF	NF	NS
1,4-Dioxane	441	441	432	445	430	553
THF	445	445	433	455	441	578
Ethyl acetate	444	441	437	450	437	580
DCM	444	449	444	460	443	NF
DMF	468	459	449	480	452	NF
tert-Butanol	464	458	458	490	466	540
Acetonitrile	478	470	464	490	464	NF
2-Propanol	475	469	459	494	464	538
1-Butanol	478	472	465	494	470	537
Ethanol	490	482	470	501	480	498
Methanol	499	497	487	503	492	NF
Ethylene glycol	505	502	492	515	495	NF
Water	515	513	511	512	515	520

[a] Solvents are listed in order of increasing dielectric constant values

[b] No fluorescence in this solvent

[c] Not soluble in this solvent

[d] Not used in dipole moment calculation and Kamlet-Taft treatment due to non-fluorescent nature

molecule. No clear transitions of n–π* type have been observed, since they are possibly masked by the more intense π–π* type transition ($\in \approx 10^4$ $M^{-1}cm^{-1}$) [73]. Assignment of A4 as CT transition is based on the presence of red-shifted band, on increasing the solvent polarity (Table 2).

Absorption spectral data suggest the ground-state structure in all the molecules to be strongly sensitive to solvent environment. As the polarity of the solvent is increased from n-hexane to water, the absorption profile becomes broad and structureless, suggesting larger solute-solvent interactions in highly polar solvents. Attention is focused on the highly red-shifted intense long-wavelength band A4 observed for the same molecule in different solvents ($\lambda_{n-hexane} = 346nm - \lambda_{water} = 391nm$), which has been assigned to charge transfer from the donor groups (>N-H, R = OH, OMe, etc., Fig. 1) to the carbonyl group.

In compound **OH-I**, for instance, absorption maxima of band A4, in methanol, ethanol, propanol and butanol is at 385, 388, 390 and 392 nm, respectively. This suggests the occurrence of a substantial increase in delocalization of charge with ionization of the hydroxyl group caused by the increase in the solvent's basicity [74]. Thus, in hydroxylic solvents the contribution of the charge from the ionized hydroxyl (conjugate base) causes extra charge transfer [compare λ_{A4} (ethanol) = 388 nm vs. λ_{A4} (acetonitrile) = 370 nm, Table 2].

Emission Properties

The longest wavelength absorption maxima band (A4) was used as excitation wavelength to record the emission spectra. For all derivatives of the indole chalcones, a completely non-structured intense band was observed in all solvents in the range of 430–580 nm (Fig. 2b). Fluorescence intensity was enhanced in polar solvents as compared to the nonpolar solvents. Fluorescence was almost absent in highly nonpolar solvents (n-hexane and cyclohexane). Fluorescence intensity in ethylene glycol was two-three times greater than in other solvents. Thus, the fluorescence intensity that was dissipated in other solvents remained unaffected in ethylene glycol due to the viscous medium.

On increasing solvent polarity, the emission became structureless and an appreciable bathochromic shift was detected with a band enlargement (Table 3). Such a behavior indicated the stabilization of the highly dipolar excited state in polar solvents.

The emission maximum of **I** derivative underwent a red shift of 74 nm on changing the solvent from 1,4-dioxane to water (Fig. 4). A considerable red shift of the spectral position for these derivatives, and the increase of the Stokes-shifts and emission bandwidth with increasing solvent polarity, point towards the distinct charge-transfer character of the fluorescent states. These effects clearly indicate the values of the excited-state dipole moments to be higher than those of the ground state (Section Excited State Dipole Moments). This behaviour points to a strong intramolecular charge transfer (ICT) character of the excited state.

Looking at the molecular structure of these derivatives, one can see that it has electron donor and acceptor pairs offering two resonating structures (structures 'A' and 'B', Fig. 5), as a result of the ICT. The resonance structure 'A' is characterized by the participation of the electron lone pair of N atom of the chromophore towards carbonyl group and the structure 'B' shows the donation of electron density from phenyl ring to the carbonyl group.

The effect of electron withdrawing substituents on **I** derivatives can be clearly seen in the cases of **Cl-I** and **NO_2-I**, as they show bathochromic shifts as compared to other derivatives in absorption and fluorescence spectra.

The lack of fluorescence in nitro derivative can be explained on the basis of the strong electron-withdrawing capacity of the nitro group (Table 3). Aromatic nitro compounds are in general only weakly fluorescent or completely nonfluorescent, due to the efficient nonradiative decay processes such as singlet-triplet intersystem crossing and internal conversion [75].

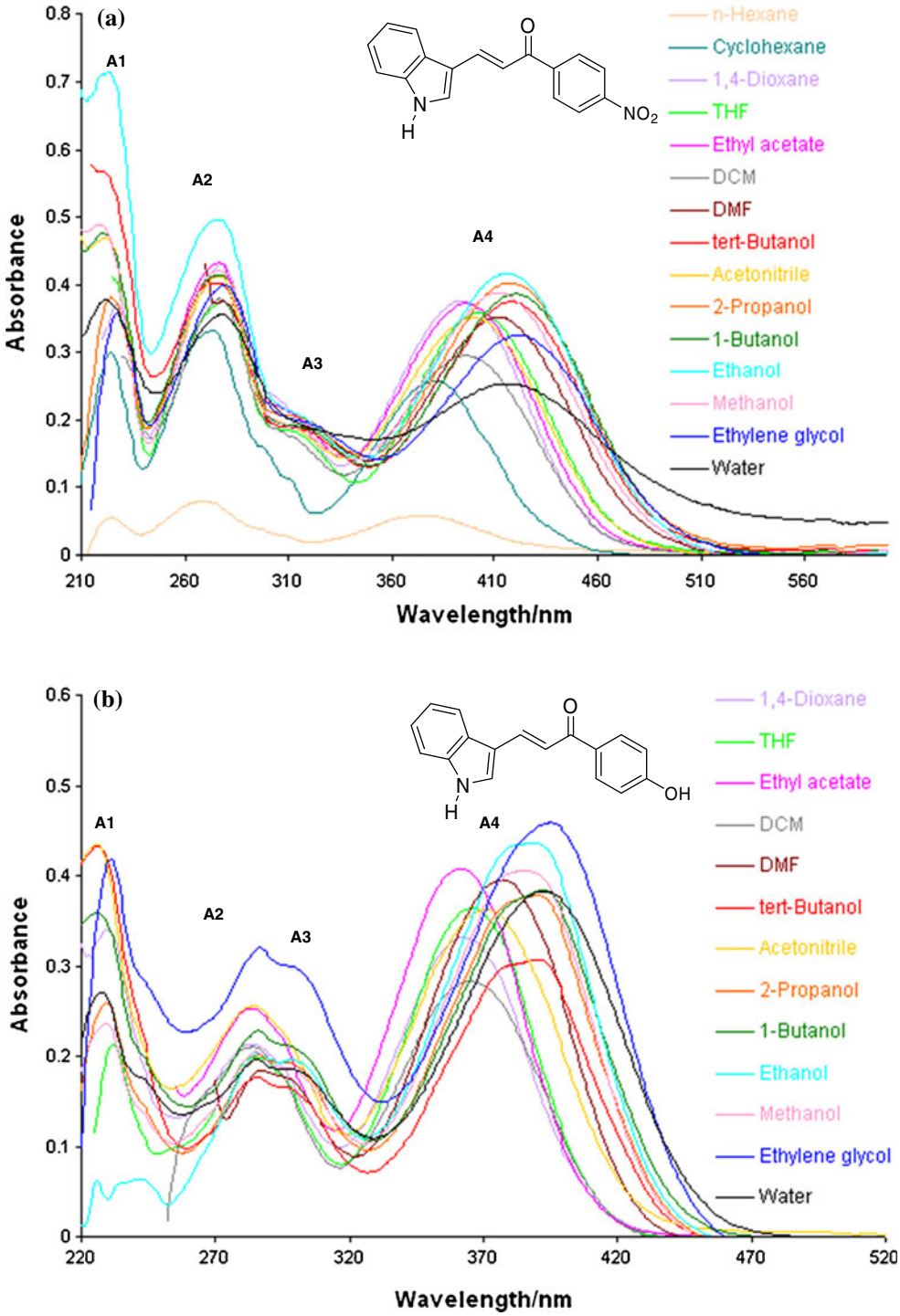

Fig. 3 **a** Electronic absorption spectra of **NO_2-I** in different solvents. **b** Electronic absorption spectra of **OH-I** in different solvents

Excited State Dipole Moments

Solvatochromic shifts caused by general (non-specific) solvent effects are often described by solvatochromic method, which relates the energy difference between absorption and emission maxima to the dielectric constant and refractive index.

The solvatochromic method has been used for the determination of the difference in the dipole moment between the ground and excited states. For estimation of the excited state dipole moments, Stokes-shifts have been calculated for all the molecules from their absorption (band λ_{A4} in Table 2) and fluorescence maxima (Table 3) in different solvents. The data in hydroxylic solvents were excluded to avoid specific solute-solvent interactions [76, 77].

Figure 6 shows the plots of Stokes-shifts for **Me-I** versus solvent polarity functions, $F_1(D,n)$, $F_2(D,n)$ and E_T^N. The

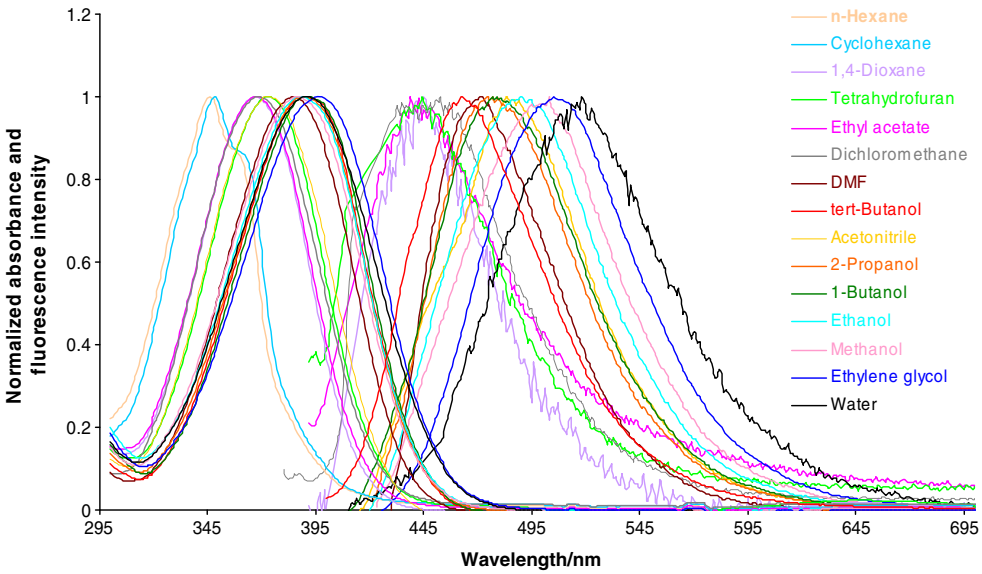

Fig. 4 Normalized absorbance and fluorescence spectra of **I**

values of correlation coefficients obtained from the linear least squares fit analysis of the Stokes-shifts versus bulk solvent polarity functions, $F_1(D,n)$ and $F_2(D,n)$ as well as microscopic solvent polarity parameter E_T^N, are summarized in Table 4.

Onsager cavity radii 'R' have been calculated theoretically in gaseous-phase for all the systems and are given in Table 5. The slopes S_1 and S_2 obtained from the plots of Eqs. 1 and 2 and the ratios of dipole moments (μ^*/μ) calculated using Eq. 6 are summarized in Table 5. The changes in dipole moment ($\Delta\mu$) values, derived from the slopes (m) obtained from the plots of Stokes-shifts versus E_T^N using Eq. 7, are given in Table 5.

The positive value of $\Delta\mu$ of all systems studied here suggests considerable amount of charge transfer from the donor to the carbonyl acceptor moieties, which leads to an increase in the polarity of the excited state and consequently, the intensification of the donor-acceptor type of intramolecular interaction.

The increase in the dipole moment values for indole chalcone derivatives upon excitation can be explained in terms of the nature of emitting state (ICT). ICT can be explained on the basis of resonance structures as shown in Fig. 5. The contributing resonance structures arise out of the delocalization of the π-electrons from either the indole or phenyl ring to the carbonyl group. The negative charge on the carbonyl favors the proposed delocalization (Fig. 5). This charge transfer accompanying excitation to lowest excited singlet-state usually results in the excited molecule having larger dipole moment than the ground-state molecule.

Resonance structures, A and B (Fig. 5), both are probable according to the structure of indole chalcones. Resonance structure 'B' dominates in the excited state with substituents having electron donating capacity (less participation of the electron lone pair of the N-atom), explaining large change in dipole moment upon excitation. Resonance structure 'A' dominates in the excited state with substituents

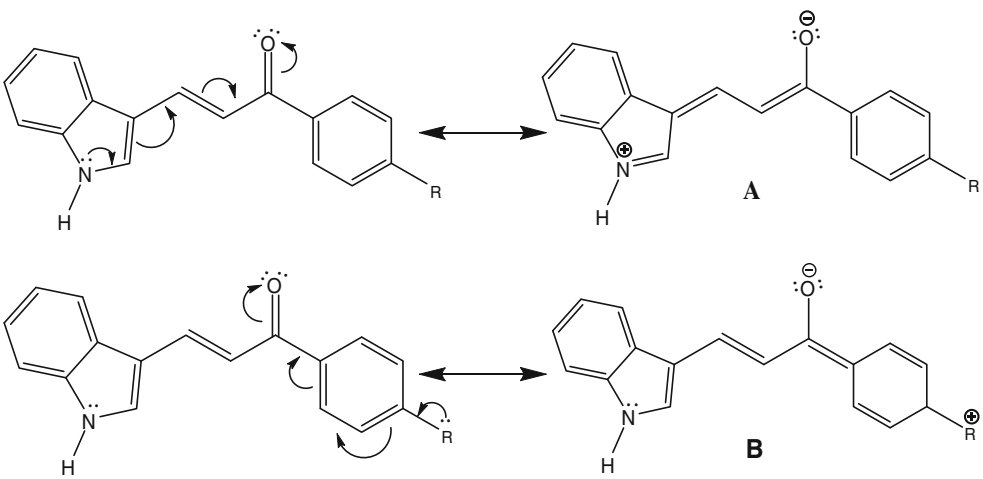

Fig. 5 Possible resonance structures of indole chalcone derivatives

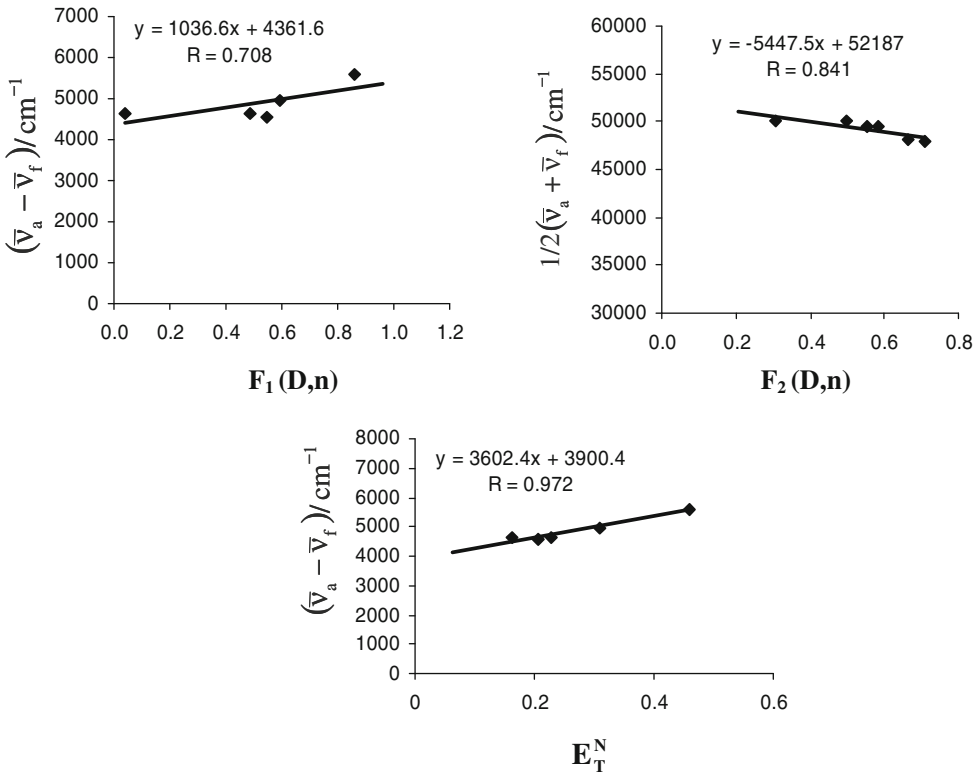

Fig. 6 Stokes-shifts for **Me-I** derivatives vs. the solvent polarity functions, F_1(D,n), F_2(D,n) and E_T^N

having electron withdrawing capacity, explaining large change in dipole moment upon excitation.

The trend observed in the values of Δμ for different **I** derivatives is in accordance with the ionization potential energies (IP) of the substituted benzene ring [78]. IP values of only those **I** derivative can relate with the Δμ values, which follow the resonance structure 'B' in the excited state. In correlation with the IP values, **OMe-I** having lowest IP value shows the highest Δμ value as compared to the other **I** derivatives. Following the trend of IP values, the **Cl-I** derivative should have lowest Δμ values but it is high and almost similar to **OMe-I**. This unusual change in the dipole moment signifies that the resonance structure formed by the **Cl-I** derivative is different from the other **I** derivatives. Thus the resonance structure 'A' dominates in the excited state of **Cl-I** derivative.

Table 4 Correlation coefficients for the fits of Stokes-shifts of indole chalcone derivatives against the solvent polarity functions, E_T^N, F_1(D,n) and F_2(D,n)

Molecule	Correlation coefficients		
	E_T^N	F_1 (D,n)	F_2 (D,n)
I	0.752	0.620	−0.813
Me-I	0.972	0.708	−0.841
OH-I	0.629	0.666	−0.855
Cl-I	0.903	0.648	−0.895
OMe-I	0.988	0.910	−0.902

There is improvement in correlation coefficients obtained for the Stokes-shifts data using E_T^N parameter (see Table 4) except for **I** and **I-OH**. Hence, the solvatochromic method based on microscopic solvent polarity parameter E_T^N seems to be more reliable in estimating excited state dipole moments than the one involving solvent polarity functions F_1(D,n) and F_2(D,n).

Kamlet and Taft Treatment

The distinct solvatochromic behavior of all **I** derivatives in protic and non-protic media must reflect different solvent effects in these environments. The absorption and emission wavelength maxima obtained in various solvents have been analyzed using the Kamlet and Taft treatment [63]. This approach separates the dielectric effects of solvents (π*), hydrogen-bond donor ability (α), and hydrogen-bond acceptor ability (β) of the solvents on the spectral properties.

Figure 7 shows the possible specific solute-solvent interactions of indole chalcone derivatives. To get information about the various solute-solvent interactions that control the solvent-induced spectral shifts, the effect of solvents on the absorption and emission energies is quantified by the multiple regressions and the results are presented in Tables 6 and 7.

The formation of various specific hydrogen bonds between the solvent and the solvatochromic probe may possibly explain the UV–vis shifts. The contribution of each of the specific interactions (solvent-carbonyl oxygen

Table 5 The change (Δμ) and the ratio (μ*/μ) of dipole moments of indole chalcones

Molecule	S_1[a]	$-S_2$[b]	Longest axis/Å	Cavity radius,[c] R/Å	Slope, m[d]	IP[e]/eV	(μ*/μ)[f]	Δμ[g]/D
I	1304	6425	9.74	3.90	3714	9.24	1.51	2.57
Me-I	1037	5447	10.85	4.34	3602	8.83	1.47	2.97
OH-I	1062	5504	10.62	4.25	2522	8.49	1.48	2.41
Cl-I	1452	7108	11.60	4.64	5263	9.07	1.51	3.98
OMe-I	1270	6144	11.80	4.72	3496	8.22	1.52	3.32
NO_2-I[h]	–	–	–	–	–	–	–	–

[a] Calculated from the plots of Stokes-shifts versus F_1 (D,n) using Eq. 1

[b] Calculated from the plots of Stokes-shifts versus F_2 (D,n) using Eq. 2

[c] Onsager cavity radius (40% of the longest axis in the optimized geometry of the molecule) obtained by using semiempirical calculations [61]

[d] Slope (m) = $11307.6[(\Delta\mu/\Delta\mu_B)^2 (R_B/R)^3]$, calculated from the plot of Stokes-shifts vs. E_T^N using Eq. 7

[e] Ionization Energies (IP) of gas-phase molecules of substituted benzene ring

[f] Calculated using Eq. 6 from experimental values of S_1 and S_2

[g] Calculated using Eq. 7 from experimental value m

[h] Not used in dipole moment calculation and Kamlet-Taft treatment due to non-fluorescent nature

atom, solvent/indole ring nitrogen atom and solvent-indole ring hydrogen atom) can have a different effect by changing the nature and geometry of the solvent [79]. This behavior explains the average correlation coefficients of the multiple square analyses, because each solvent most likely interacts in a different way with the probe (>NH and > C = O).

The possible hydrogen bonds involved in the ground and the excited states of **I** derivatives are shown in Fig. 8. These derivatives can accept hydrogen bonds at the nitrogen lone pair (type X) and at the carbonyl group (type Z) from hydrogen bond donating solvents. These derivatives can also show hydrogen bond formation with hydrogen bond accepting solvents from the H atom on the NH group (type Y) [80].

The negative values of **a**, **b** and **s** indicate that all the three parameters π*, α and β, contribute to the stabilization of the ground state as well as the excited state (Tables 6 and 7) [81].

Excitation Process

The more negative values of **b** point toward the higher HBD ability of the molecules, as the lone pair of electrons of N atom in indole ring participates in the formation of hydrogen bond with solvents. The lower negative value of **a** for all the derivatives designates the lowest HBA ability (Table 6) [76, 82].

For all the derivatives, there is a stabilizing term **b** for the ground state caused by donating hydrogen bonds from the NH group (Table 6) [81]. This is due to the two factors, first is the weak strength of the hydrogen bond of type X and type Z and second is the strong hydrogen bond strength of type Y (Fig. 8) [80].

Emission Process

The more negative values of **a** in emission process as compared to the excitation process reveal that the HBA ability is more in excited state [76, 81]. This is because of the strengthening of the hydrogen bond on the carbonyl group (type Z). Hydrogen bond of type Z is thus stronger than the hydrogen bonds of type X and type Y (Fig. 8 and Table 7) [80].

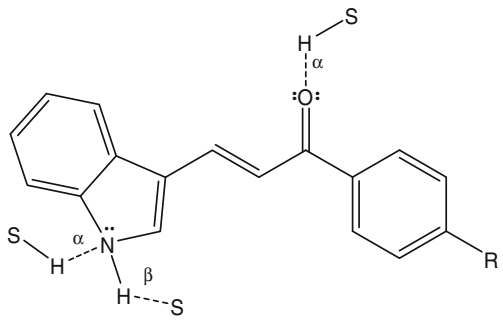

Fig. 7 Possible specific solute-solvent interactions of indole chalcone derivatives (S and HS = Solvent)

Table 6 Multiparametric correlation of Kamlet-Taft parameters using the LSER equation, $\nu = \nu_o + s\pi^* + a\alpha + b\beta$ towards the spectral properties of indole chalcone derivatives in excitation processes

Molecule	ν_o	a	b	s	r[a]
I	28803	−654	−2203	−1573	0.979
Me-I	28948	−824	−2090	−1651	0.977
OH-I	28836	−1232	−2015	−1090	0.940
Cl-I	28280	−522	−2334	−1728	0.979
OMe-I	29052	−1058	−2386	−1411	0.974

[a] Correlation coefficients of indole chalcones in their respective LSER equations

Table 7 Multiparametric correlation of Kamlet-Taft parameters using the LSER equation, $\nu = \nu_o + s\pi^* + a\alpha + b\beta$ towards the spectral properties of indole chalcone derivatives in emission processes

Molecule	ν_o	a	b	s	r[a]
I	24007	−1697	−1025	−2187	0.902
Me-I	23596	−1848	−247	−1887	0.937
OH-I	23927	−1938	−140	−1890	0.924
Cl-I	23535	−1437	−1636	−1845	0.864
OMe-I	24124	−1958	−706	−1929	0.930

[a] Correlation coefficients of indole chalcones in their respective LSER equations

The more negative values of **b** in case of **Cl-I** show that the HBD ability is more in excited state, thus favoring structure 'A' as compared to the other derivatives with the less negative value of **b**, thus favoring structure 'B' in excitation process (Fig. 5 and Table 7). On comparing the values of **b** for all the derivatives in excitation process, the **OH-I** shows the lowest negative value of **b** because of electron donating tendency of both NH and OH groups (Table 7) [80, 81].

In emission process, the large negative values of **s** of these compounds indicate that excited state has large ICT character. The absolute value of **s** shows that excited state is more polar and sensitive to the environment than the ground state as evident from μ*/μ and Δμ values (Tables 5 and 7).

Conclusions

The photophysical properties of these indole chalcone derivatives are reported and discussed by examining solvent effects on the absorption and fluorescence spectra. These derivatives show positive solvatochromism with the increase in the polarity of the solvent. This study has brought into focus the single emission that originates from ICT excited states. The changes displayed by the photophysical properties of this molecule in different solvents can be explained in terms of electron distribution and hydrogen bonding participation in the stabilization of these molecules in ground and excited states.

In the LSER equation, parameters α, β and π* play important roles in the mechanism of the interactions between these probes and solvents. These derivatives show hydrogen bond accepting ability in ground state and hydrogen bond donating ability in excited state. The lowest singlet excited state of these molecules has larger dipole moment than that of the ground state. Based on multiparametric regression analysis, it appears that the excited state stabilization is mainly determined by the dipolar interactions and hydrogen bond accepting ability of solvents. Dipolar interaction contributes usually to high value of μ*/μ and Δ μ more in the excited state than in the ground state.

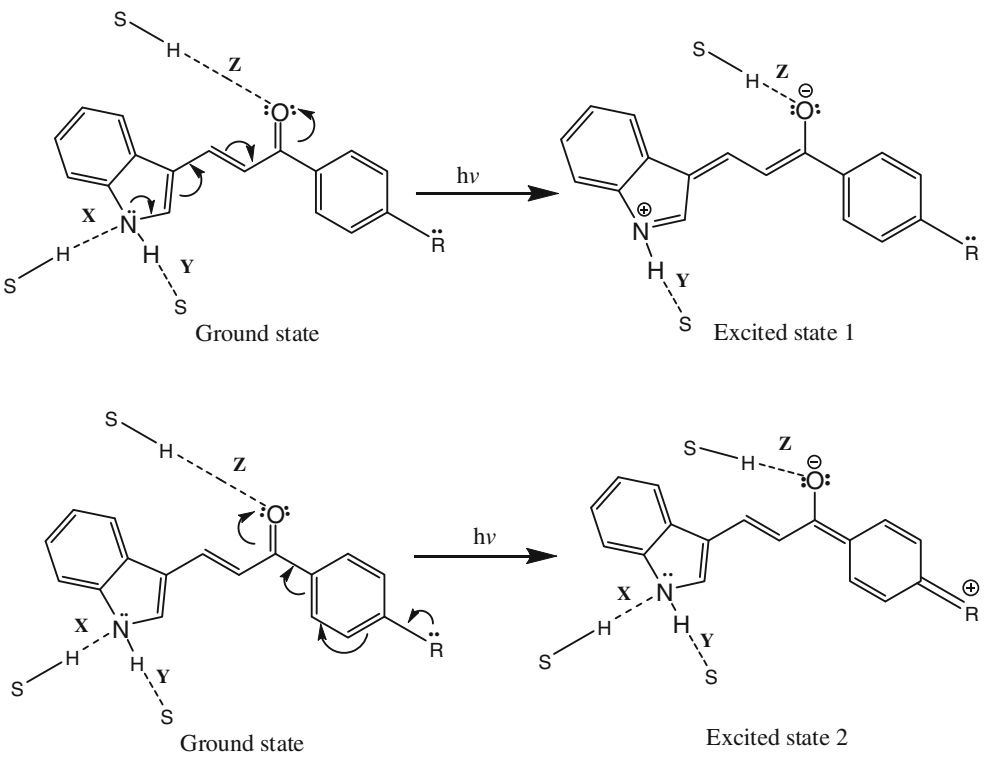

Fig. 8 Simplified view of the possible hydrogen bonds involved in the ground and the excited states of **I** derivatives. Hydrogen bonds may be formed on the nitrogen lone pair (type X) and the carbonyl group (type Z) from hydrogen bond donating solvents, and hydrogen atoms on the NH group (type Y) from hydrogen bond accepting solvents (S and HS = Solvent)

Acknowledgements The financial support from University of Delhi under the Scheme "To strengthen R & D Doctoral Research Program" is gratefully acknowledged. Manju K. Saroj is thankful to the University Grants Commission (UGC), New Delhi for the financial assistance. The authors thank the Institute of Genomics and Integrative Biology (IGIB, CSIR), Delhi for providing access to its Central Instrumentation Facility.

References

1. Eisenhart JM, Ellis AB (1985) Perturbation of the excited-state properties of trans, trans-1,5-bis[4-(dimethylamino) phenyl]-1,4-pentadien-3-one through adduct formation and silica gel adsorption. J Org Chem 50(21):4108–4113
2. Jiang YB, Wang XJ, Lin L (1994) Fluorescent probing of the restriction by aqueous micelles of the formation of the photoinduced biradical state P^* of 4-(dimethy1amino) chalcone. J Phys Chem 98(47):12367–12372
3. Wang P, Wu S (1995) Spectroscopy and photophysics of bridged enone derivatives: effect of molecular structure and solvent. J Photochem Photobiol A Chem 86(1–3):109–113
4. Matsushima R, Mizuno H, Itoh H (1995) Photochromic properties of 4′-amino-substituted 2-hydroxychalcones. J Photochem Photobiol A Chem 89(3):251–256
5. Gaber M, El-Sayed YS, Diab H (2011) Spectral behavior study of 3-(4-dimethylamino-phenyl)-1-6-[3-(4-dimethylamino-phenyl)-acryloyl]-pyridin-2-yl- propanone. Opt Laser Technol 43(3):592–598
6. Nielsen SB, Christensen SF, Cruciani G, Kharazmi A (1998) Antileishmanial chalcones: statistical design, synthesis and three-dimensional quantitative structure-activity relationship analysis. J Med Chem 41(24):4819–4832
7. Liu X, Go ML (2007) Antiproliferative activity of chalcones with basic functionalities. Bioorg Med Chem 15(22):7021–7034
8. Batovska D, Parushev S, Stamboliyska B, Tsvetkova I, Ninova M, Najdenski H (2009) Examination of growth inhibitory properties of synthetic chalcones for which antibacterial activity was predicted. Eur J Med Chem 44(5):2211–2218
9. Perez-Vizcaino F, Duarte J (2010) Flavonols and cardiovascular disease. Mol Aspect Med 31(6):478–494
10. Song DM, Jung KH, Moon JH, Shin DM (2002) Photochemistry of chalcone and the application of chalcone-derivatives in photo-alignment layer of liquid crystal display. Opt Mater 21(1–3):667–671
11. Shin DM, Song DM, Kim YB (2004) Photochemical reaction on the polymer layer for liquid crystal display. Mater Sci Eng C 24(1–2):127–130
12. Guo M, Wang X (2009) Polyimides with main-chain photosensitive groups: synthesis, characterization and their properties as liquid crystal alignment layers. Eur Polym J 45(3):888–898
13. El-Sayed YS, El-Daly SA, Gaber M (2010) Spectral behavior and laser activity of 3-(4′-dimethylaminophenyl)-1-(1H-pyrrol-2-yl) prop-2-en-1-one (DMAPrP) a new laser dye. Opt Laser Technol 42(2):397–402
14. Meric B, Kerman K, Ozkan D (2002) Electrochemical biosensor for the interaction of DNA with the alkylating agent 4,4′-dihydroxy chalcone based on guanine and adenine signals. J Pharm Biomed Anal 30(4):1339–1346
15. Keri RS, Hosamani KM, Shingalapur RV, Hugar MH (2010) Analgesic, anti-pyretic and DNA cleavage studies of novel pyrimidine derivatives of coumarin moiety. Eur J Med Chem 45(6):2597–2605
16. Morkunas I, Narozna D, Nab W, Nowak SS, Remlein-Starosta D (2011) Cross-talk interactions of sucrose and fusarium oxysporum in the phenylpropanoid pathway and the accumulation and localization of flavonoids in embryo axes of yellow lupine. J Plant Physiol 168(5):424–433
17. Marcotte N, Ferry-Forgues S, Lavabre D (1999) Spectroscopic study of a symmetrical bis crown fluoroionophore of the diphenylpentadienone series. J Phys Chem A 103(17):3163–3170
18. Rurack K, Bricks JL, Reck G, Radeglia R, Resch-Genger U (2000) Chalcone-analogue dyes emitting in the near-infrared (NIR): influence of donor-acceptor substitution and cation complexation on their spectroscopic properties and x-ray structure. J Phys Chem A 104(14):3087–3109
19. Ichimura C, Shiraishi Y, Hirai T (2011) Cu (II)-selective fluorescence of a bis-quinolylimine derivative. J Photochem Photobiol A Chem 217(1):253–258
20. Kumar D, Kumar NM, Akamatsu K, Kusaka E, Harada H, Ito T (2010) Synthesis and biological evaluation of indolyl chalcones as antitumor agents. Bioorg Med Chem Lett 20(13):3916–3919
21. Rani P, Srivastava VK, Kumar A (2004) Synthesis and antiinflammatory activity of heterocyclic indole derivatives. Eur J Med Chem 39(5):449–452
22. Maria K, Dimitra HL, Maria G (2008) Synthesis and anti-inflammatory activity of chalcones and related mannich bases. Med Chem 4(6):586–596
23. Cocconcelli G, Diodato E, Caricasole A, Gaviraghi G, Genesio E, Ghiron C, Magnoni L, Pecchioli E, Plazzib PV, Terstappen GC (2008) Aryl azoles with neuroprotective activity-parallel synthesis and attempts at target identification. Bioorg Med Chem 16(4):2043–2052
24. Budakoti A, Bhat AR, Athar F, Azam A (2008) Syntheses and evaluation of 3-(3-bromo phenyl)-5-phenyl-1-(thiazolo [4,5-b] quinoxaline-2-yl)-2-pyrazoline derivatives. Eur J Med Chem 43(8):1749–1757
25. Cui M, Ono M, Kimura H, Liu BL, Saji H (2011) Synthesis and biological evaluation of indole-chalcone derivatives as β-amyloid imaging probe. Bioorg Med Chem Lett 21(3):980–982
26. Gaikwad P, Priyadarsini KI, Naumov S, Rao BSM (2010) Radiation and quantum chemical studies of chalcone derivatives. J Phys Chem A 114(30):7877–7885
27. Yesuthangam Y, Pandian S, Venkatesan K, Gandhidasan R, Murugesan R (2011) Photogeneration of reactive oxygen species and photoinduced plasmid DNA cleavage by novel synthetic chalcones. J Photochem Photobiol B Biol 102(3):200–208
28. Lakowicz JR (2006) Principles of fluorescence spectroscopy, 3rd edn. Plenum, New York
29. Sowmiya M, Tiwari AK, Saha SK (2011) Study on intramolecular charge transfer fluorescence properties of trans-4-[4′-(N, N′-dimethylamino) styryl] pyridine: effect of solvent and pH. J Photochem Photobiol A Chem 218(1):76–86
30. Melavanki RM, Patil NR, Kapatkar SB, Ayachit NH, Umapathy S, Thipperudrappa J, Nataraju AR (2011) Solvent effect on the spectroscopic properties of 6MAMC and 7MAMC. J Mol Liq 158(2):105–110
31. Tsukerman SV, Bugai AI, Lavrushin VF (1972) Electronic spectra of α, β-unsaturated ketones–indole derivatives. Khim Geterotsikl Soedin 7:949–953
32. Fuini JF, Surampudi AB, Penick MA, Mahindaratne MPD, Negrete GR, Brancaleon L (2011) The photophysical characterisation of novel 3,9-dialkyloxy- and diacyloxyperylenes. Dye Pigment 88(2):204–211
33. Guzow K, Szabelski M, Karolczak J, Wiczk W (2005) Solvatochromism of 3-[2-(aryl) benzoxazol-5-yl]alanine derivatives. J Photochem Photobiol A Chem 170(3):215–223
34. Sharma VK, Sahare PD, Rastogi RC (2003) Excited state characteristics of acridine dyes: acriflavine and acridine orange. Spectrochim Acta A 59(8):1799–1804

35. Sharma N, Jain SK, Rastogi RC (2003) Excited-state dipole moments of indoles using solvatochromic shift methods: an experimental and theoretical study. Bull Chem Soc Jpn 76 (9):1741–1746
36. Kumar S, Rao VC, Rastogi RC (2001) Excited-state dipole moments of some hydroxyl coumarin dyes using an efficient solvatochromic method based on the solvent polarity parameter E_T^N. Spectrochim Acta A 57(1):41–47
37. Kumar S, Jain SK, Sharma N, Rastogi RC (2001) Intramolecular excited-state proton-transfer studies on flavones in different environments. Spectrochim Acta A 57(2):299–308
38. Kumar S, Jain SK, Rastogi RC (2001) An experimental and theoretical study of excited-state dipole moments of some flavones using an efficient solvatochromic method based on the solvent polarity parameter E_T^N. Spectrochim Acta A 57(2):291–298
39. Dash N, Krishnamoorthy G (2010) Photophysics of 2-(4′-N, N-dimethylaminophenyl) imidazo [4,5-b] pyridine in micelles: selective dual fluorescence in sodium dodecylsulphate and triton X-100. J Fluoresc 20(1):135–142
40. Sharma N, Jain SK, Rastogi RC (2008) Solubilization of 5-methoxy tryptamine molecular probes in CTAB and SDS micelles: a CMC and binding constant study. Spectrochim Acta A 69 (3):748–756
41. Sharma N, Jain SK, Rastogi RC (2007) Effect of CTAB and SDS micelles on the excited state equilibria of some indole probes. Spectrochim Acta A 68(3):927–941
42. Tsukerman SV, Bugai AI, Nikitchenko VM, Lavrushin VF (1970) Synthesis of unsaturated ketones and derivatives of 2-pyrazoline containing an indole nucleus. Khim Geterotsikl Soedin 6(3):399–403
43. Bilot L, Kawski A (1962) Theory of the effect of solvents on the electron spectra of molecules. Z Naturforsch 17a:621–627
44. Bilot L, Kawski A (1963) Effect of the solvent on the electronic spectrum of luminescent molecules. Z Naturforsch 18a:10–15
45. Bilot L, Kawski A (1963) Dipole moments of some phthalimide derivatives in the first excited singlet state. Z Naturforsch 18a:256
46. Kawski A (1992) Progress in photochemistry and photophysics, vol. V. CRC, Boca Raton, pp 1–47
47. Kawski A (1964) Effect of polar molecules on electronic spectrum on 4-amino-phthalimide. Acta Phys Polon 25(2):285–290
48. Kawski A (1965) Abnormal stokes shift of the absorption and of the fluorescence maximum of 4-aminophthalimide in dioxane-water mixtures. Acta Phys Polon 28(5):647–652
49. Kawski A, Stefanowska U (1965) The anomalous red shift of the absorption and fluorescence spectra of 4-aminophthalimide in dependence on the ratio of homo- and heteropolar solvents. Acta Phys Polon 28(6):809–822
50. Kawski A (2002) On the estimation of excited-state dipole moments from solvatochromic shifts of absorption and fluorescence spectra. Z Naturforsch 57a(5):255–262
51. Kawski A, Kuklinski B, Bojarski P (2007) Excited state dipole moments of 4-(dimethylamino)benzaldehyde. Chem Phys Lett 448(4–6):208–212
52. Ooshika Y (1954) Absorption spectra of dyes in solution. J Phys Soc Japan 9(4):594–602
53. McRae EG (1957) Theory of solvent effects on molecular electronic spectra frequency shifts. J Phys Chem 61:562–572
54. Lippert E (1957) Spectroscopic determination of the dipole moment of aromatic compounds in the first excited singlet state. Z Elektrochem Angew Phys Chem 61:962–975
55. Bakhshiev NG (1961) Universal intermolecular interactions and their effect on the position of the electronic spectra of the molecules in two-component solutions. I. Theory (liquid solutions). Opt Spectrosc 10:717–726
56. Bakhshiev NG (1964) Universal intermolecular interactions and their effect on the position of the electronic spectra of molecules in two-component solutions VII theory (general case of an isotropic solution). Opt Spectrosc 16(5):821–832
57. Liptay W (1965) Solvent–dependence of the wave number of electron bands and physicochemical fundamentals. Z Naturforsch 20a(11):1441–1471
58. Ravi M, Samanta A, Radhakrishnan TP (1994) Excited state dipole moments from an efficient analysis of solvatochromic stokes shift data. J Phys Chem 98(37):9133–9136
59. Reichardt C (1988) Solvents and solvent effects in organic chemistry. VCH, Weinheim
60. Reichardt C (1994) Solvatochromic dyes as solvent polarity indicators. Chem Rev 94(8):2319–2358
61. Hermant RM, Bakker NAC, Scherer T, Krijnen B, Verhoeven JW (1990) Systematic study of a series of highly fluorescent rod-shaped donor-acceptor systems. J Am Chem Soc 112(3):1214–1221
62. HyperChem Release 5.1, Hypercube, Inc, USA, 1997
63. Kamlet MJ, Abboud JM, Taft RW (1981) Progress in physical organic chemistry, vol. 13. Wiley, New York, pp 485–630
64. Mataga N, Kubata T (1970) Molecular interactions and electronic spectra. Marcel Dekker, New York
65. Abboud JM, Kamlet MJ, Taft RW (1977) Regarding a generalized scale of solvent polarities. J Am Chem Soc 99(25):8325–8327
66. Kamlet MJ, Taft RW (1976) The Solvatochromic comparison method. I. The β scale of solvent hydrogen-bond acceptor (HBA) basicities. J Am Chem Soc 98(2):377–383
67. Kamlet MJ, Taft RW (1979) Linear solvation energy relationships. Part 3. Some reinterpretations of solvent effects based on correlations with solvent π* and α values. J Chem Soc Perkin Trans 2(3):349–356
68. Lagalante AF, Jacobson RJ, Bruno TJ (1996) UV/Vis spectroscopic evaluation of 4-nitropyridine N-oxide as a solvatochromic indicator for the hydrogen-bond donor ability of solvents. J Org Chem 61(18):6404–6406
69. Taft RW, Abboud JLM, Kamlet MJ (1981) Linear solvation energy relationships. 12. The dδ term in the solvatochromic equations. J Am Chem Soc 103(5):1080–1086
70. Kamlet MJ, Abboud JLM, Abraham MH, Taft RW (1983) Linear solvation energy relationships. 23. A comprehensive collection of the solvatochromic parameters, π*, α and β, and some methods for simplifying the generalized solvatochromic equation. J Org Chem 48(17):2877–2887
71. Blanco SE, Ferretti FH (1998) Determination of absorptivity and formation constant of a chalcone association complex. Talanta 45 (6):1103–1109
72. Sharma N, Jain SK, Rastogi RC (2007) Solvatochromic study of excited state dipole moments of some biologically active indoles and tryptamines. Spectrochim Acta A 66(1):171–176
73. Etaiw SEH, Awad MK, Fayed TA, El-Hendawy MM (2009) Effect of N-methylation on both ground and excited states properties of 1-(9-anthryl)-2-(2-benzothiazolyl) ethane. J Mol Struct 919(1–3):12–20
74. Al-Ansari IAZ (1997) Ground- and excited-state properties of some 3,4-dihydro-1-(2-p-substituted benzylidene) naphthalenones: substituent and environmental effects. J Phys Org Chem 10(9):687–696
75. Sonoda Y, Tsuzuki S, Goto M, Tohnai N, Yoshida M (2010) Fluorescence spectroscopic properties of nitro-substituted diphenylpolyenes: effects of intramolecular planarization and intermolecular interactions in crystals. J Phys Chem A 114(1):172–182
76. Fayed TA, Awad MK (2004) Dual emission of chalcone-analogue dyes emitting in the red region. Chemical Phys 303(3):317–326
77. El-Daly SA, Gaber M, Al-Shihry SS, El Sayed YS (2008) Photophysical properties, excitation energy transfer and laser activity of 3-(4′-dimethylaminophenyl)-1-(2-pyridinyl) prop-2-en-1-one (DMAPP): a new potential laser dye. J Photochem Photobiol A Chem 195(1):89–98

78. Lide DR (ed) (2005) CRC handbook of chemistry and physics, 85th edn. CRC, Boca Raton, pp 10–193
79. Bolz I, May C, Spange S (2007) Solvatochromic properties of Schiff bases derived from 5-aminobarbituric acid: chromophores with hydrogen bonding patterns as components for coupled structures. New J Chem 31(9):1568–1571
80. Gustavsson T, Cassara L, Gulbinas V, Gurzadyan G, Mialocq JC, Pommeret S, Sorgius M, Meulen PV (1998) Femtosecond spectroscopic study of relaxation processes of three amino-substituted coumarin dyes in methanol and dimethyl sulfoxide. J Phys Chem A 102(23):4229–4245
81. Saha SK, Purkayastha P, Dasb AB (2008) Photophysical characterization and effect of pH on the twisted intramolecular charge transfer fluorescence of trans-2-[4-(dimethylamino) styryl] benzothiazole. J Photochem Photobiol A Chem 195(2–3):368–377
82. Li M, Huangb J, Zhoub X, Luoa H (2010) Synthesis, characterization and spectroscopic investigation of a novel phenylhydrazone schiff base with solvatochromism. Spectrochim Acta A 75(2):753–759